CHAPTER VII

WIRELINE FORMATION TEST IN SINGLE LAYER RESERVOIR WITH STIMULATED ZONE

A single layer reservoir with stimulated zone due to well stimulation is investigated in order to evaluate the effects of mobility ratio and effects of radius of stimulated zone. The increasing in permeability of a zone around the well causes the skin effect. Simulations and interpretations are performed under different scenarios to see whether wireline formation testing with a single probe can be used to evaluate reservoir properties of a stimulated reservoir. The grid sizes of the reservoir model are the same as those in the base case and so are the reservoir conditions and fluid properties. The reservoir model has two zones as shown in Figure 7.1. The permeability anisotropy ratio for each zone is kept constant at 0.1. Two different sets of damaged and undamaged permeability are used. In each set, the effects of mobility ratio and effects of radius of invasion are studied.

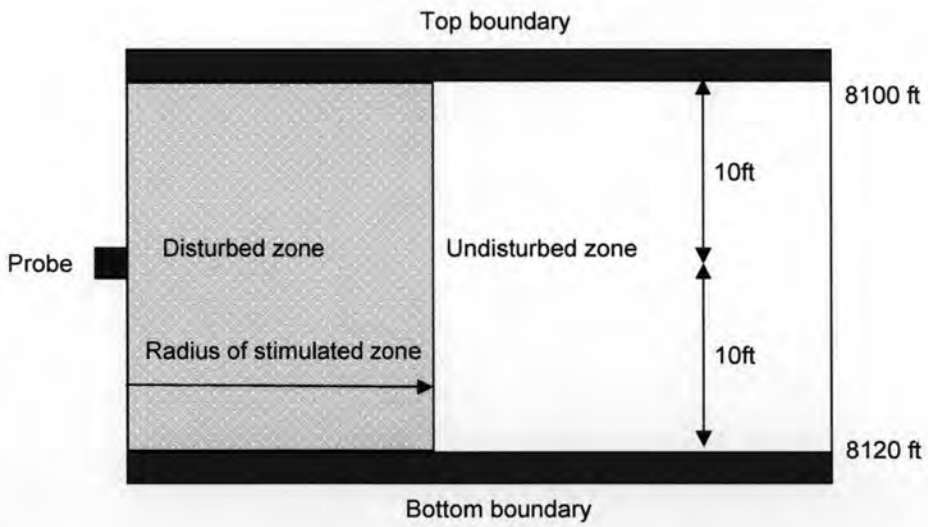

Figure 7.1 : Schematic reservoir description for stimulated reservoir.

7.1 Case I : Undisturbed Permeability of 50 mD, Stimulated Zone Permeability of 75 mD

7.1.1 Effects of Mobility Ratio

In this case study, the objective is to investigate the effects of mobility ratio between stimulated zone and the reservoir on pressure transients by fixing the permeability of the native reservoir while varying the permeability of the stimulated zone. Three different mobility ratios, K_{hi}/K_{hu} of 1.2, 1.5, and 1.8 are considered. The native reservoir permeability is fixed at 50 mD while the stimulated zone permeability varies with the mobility ratio. The radius of stimulated zone is fixed at 1.2867 ft. away from the borehole wall as shown in Figure 7.2. The flow period consists of a 30-minute drawdown and a 90-minute buildup. After running reservoir simulation for pressure response, the data were then interpreted by pressure transient analysis technique. The pressure history and the diagnostic plots of the tests are shown in Figures 7.3 and 7.4, respectively, and the interpreted results are tabulated in Table 7.1. The regression fits to the tests are shown in Appendix B.

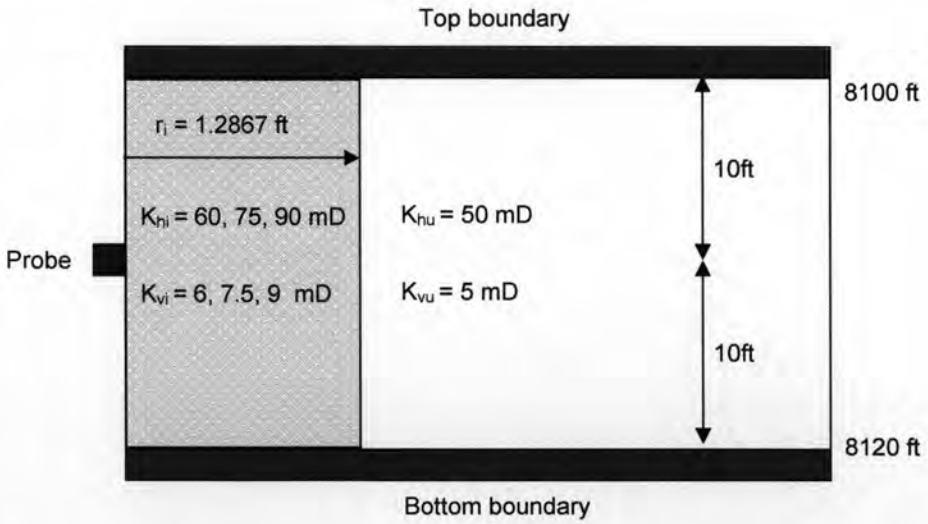

Figure 7.2 : Schematic reservoir description for different mobility ratios between stimulated zone and native reservoir for case I.

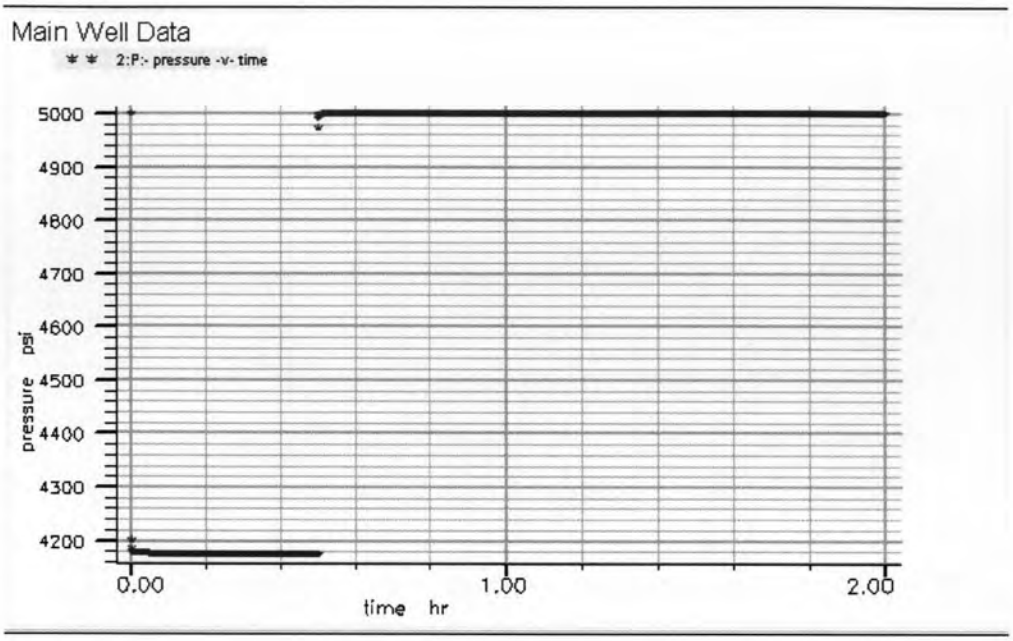

Figure 7.3 : Pressure history for case K75-50 (mobility ratio = 1.5)

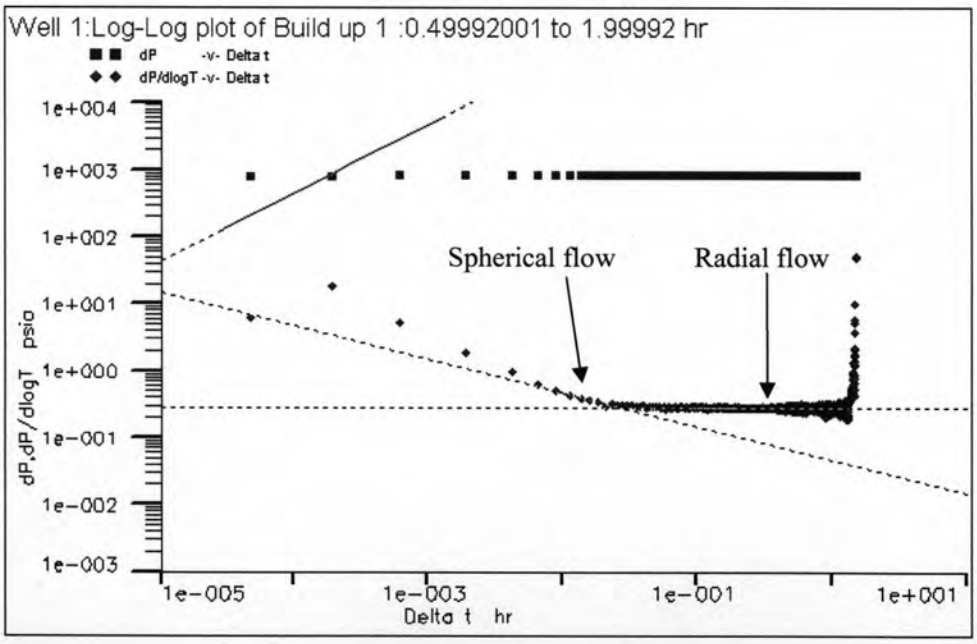

(a) Mobility ratio = 1.2

Figure 7.4 : Diagnostic plots for different mobility ratios between stimulated zone and native reservoir for case I.

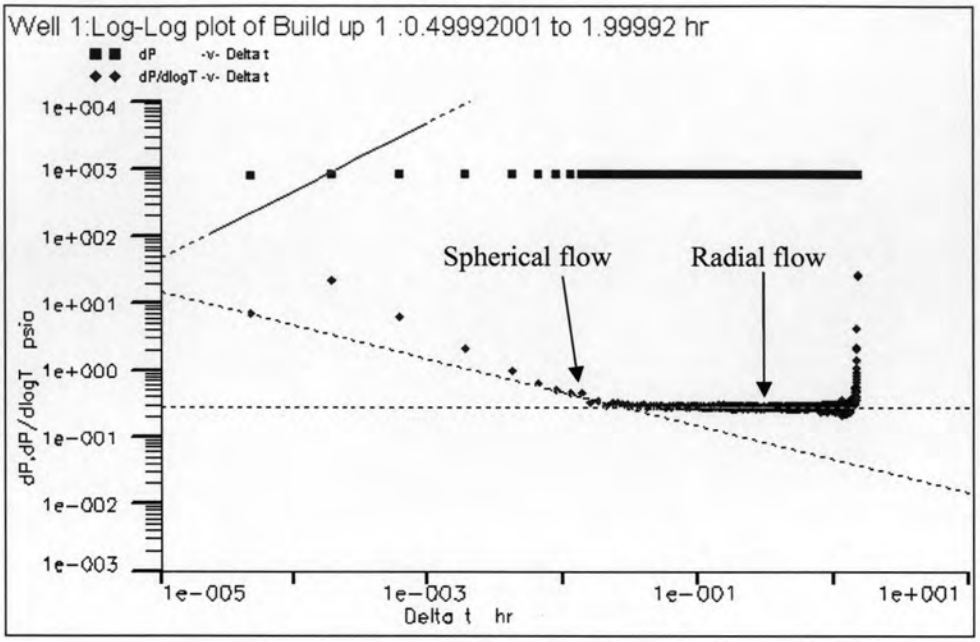

(b) Mobility ratio = 1.5

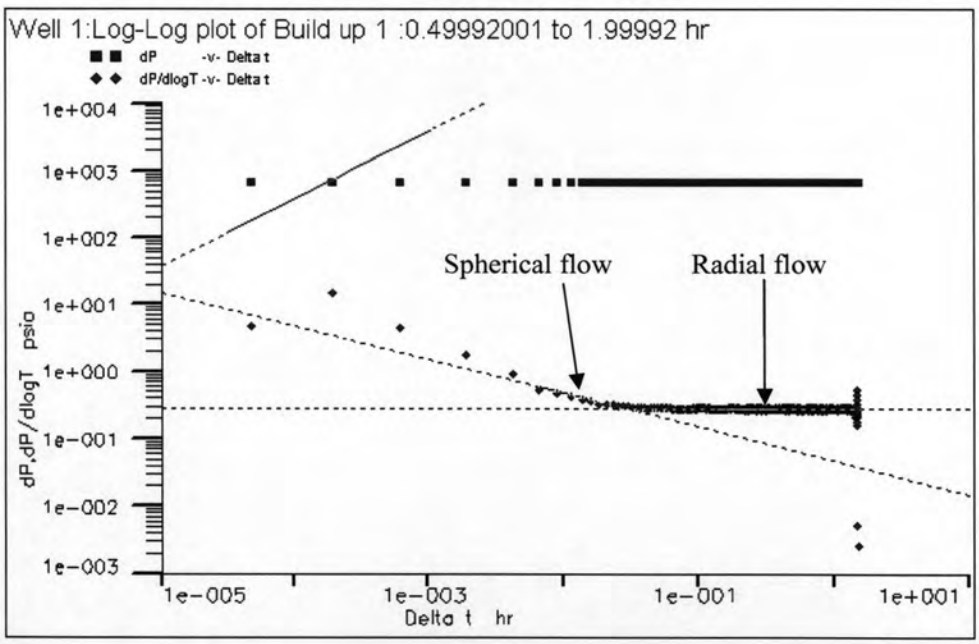

(c) Mobility ratio = 1.8

Figure 7.4 : Diagnostic plots for different mobility ratios between stimulated zone and native reservoir for case I (continued).

Table 7.1 : Interpreted results for different mobility ratios between stimulated zone and native reservoir for case I.

Case	K_{hi}	K_{hu}	S_p	S_M	S_t	Interpreted results		Error %		
	(mD)	(mD)				K_h (mD)	Skin	K_h (mD)	S_M	S_t
K60-50	60	50	0.399	-0.273	0.126	49	0.138	-2.00	150.54	9.52
K75-50	75	50	0.299	-0.546	-0.247	47.9	-0.135	-4.20	75.27	45.34
K90-50	90	50	0.119	-0.728	-0.609	53.8	-0.302	7.60	58.51	50.41

As can be seen in Figure 7.4 (a), (b), and (c), the spherical flow model and the radial flow model can be matched with the pressure derivative plot. In Appendix B, in Figure B5 (a), (b), and (c), the regression shows good consistency on the log-log diagnostic plot. The regression model is vertical interference test.

In this case study, we fixed the stimulated zone radius but varied the permeability in the stimulated zone. The effect from the permeability contrast between the native reservoir and the stimulated zone can be quantified by the skin factor. The interpreted results obtained from the regression for different mobility ratios are summarized in Table 7.1. In cases K60-50, K75-50, and K90-50, the interpreted skin factor is different from the mechanical skin factor calculated from the definition of the skin factor, with an error of 150.54, 75.27, and 58.51 %, respectively. It can be seen that the interpreted skin factor is too large compared with the mechanical skin factor. This can be concluded that the interpreted skin factor is affected by the spherical skin or the skin due to probe, S_P as can be seen that the errors between the interpreted results and the total skin factor, S_t are reduced to 9.52, 45.34, and 50.41 %, respectively. For horizontal permeability, the interpreted results are quite similar to the input value of native reservoir horizontal permeability suggesting that the interpreted horizontal permeability is not affected by the mobility ratio.

7.1.2 Effects of Radius of Stimulated Zone

In this case study, the objective is to investigate the effects of radius of the stimulated zone on pressure transients by fixing the permeability of the stimulated zone and the native reservoir while varying the stimulated zone radius as depicted in

Figure 7.5. Six different radii of stimulated zones, r_s of 0.44, 0.64, 1.28, 3.35, 4.56, and 6.19 ft. are considered. The native reservoir permeability is fixed at 50 mD, and the stimulated zone permeability is fixed at 75 mD. The flow period consists of a 30-minute drawdown and a 90-minute buildup. After running reservoir simulation for pressure response, the data were then interpreted by pressure transient analysis technique. The pressure history and the diagnostic plots of the tests are shown in Figures 7.6 and 7.7, respectively, and the interpreted results are tabulated in Table 7.2. The regression fits to the tests are shown in Appendix B.

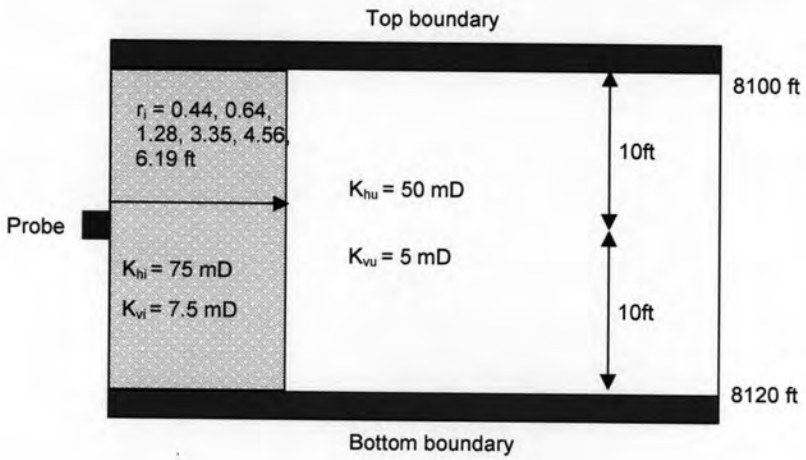

Figure 7.5 : Schematic reservoir description for different radii of stimulated zone for case I.

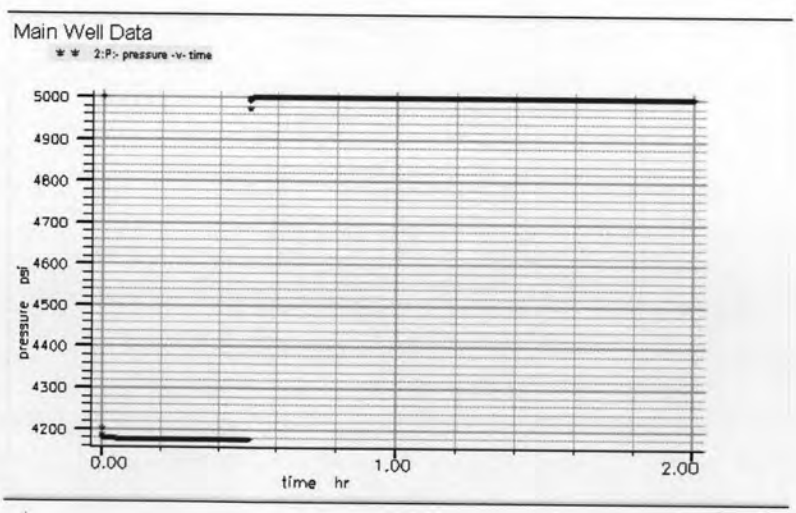

Figure 7.6 : Pressure history of case K75-50-3 (stimulated zone = 1.28 ft.)

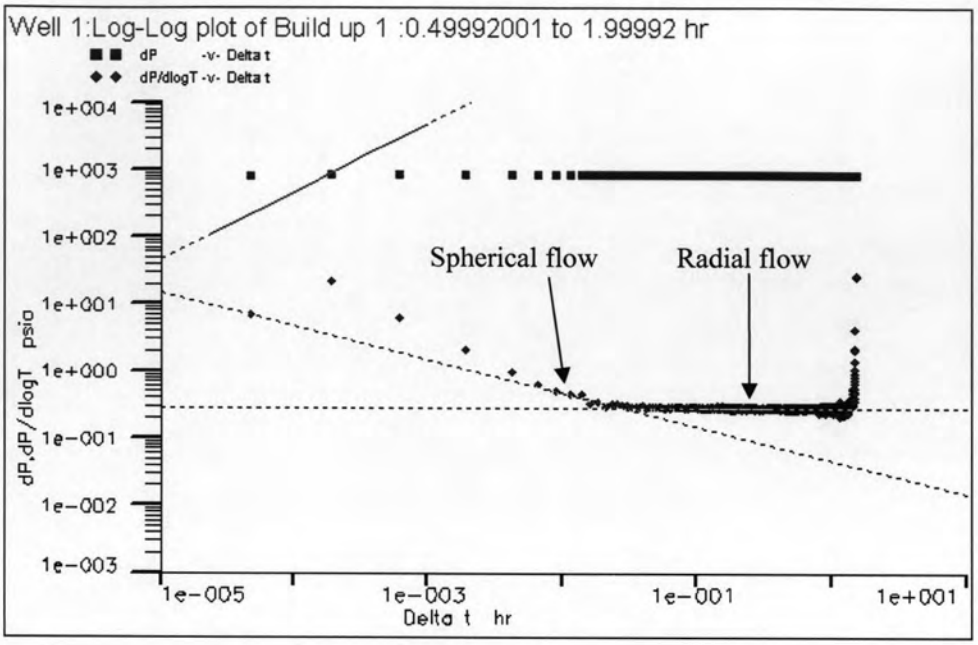

(a) Radius of stimulated zone = 0.44 ft.

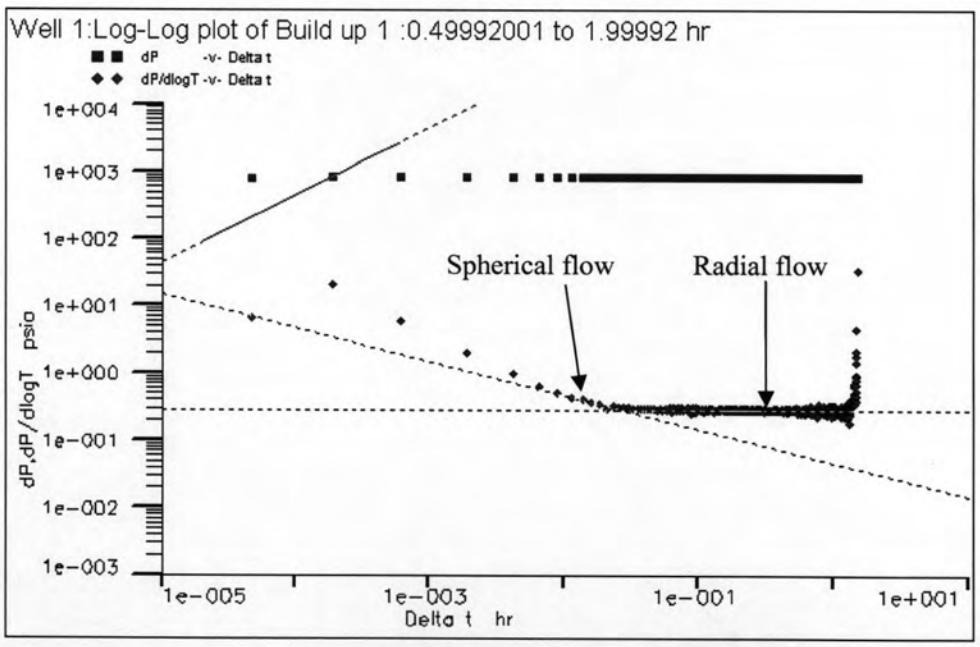

(b) Radius of stimulated zone = 0.64 ft.

Figure 7.7 : Diagnostic plots for different radii of stimulated zone for case I.

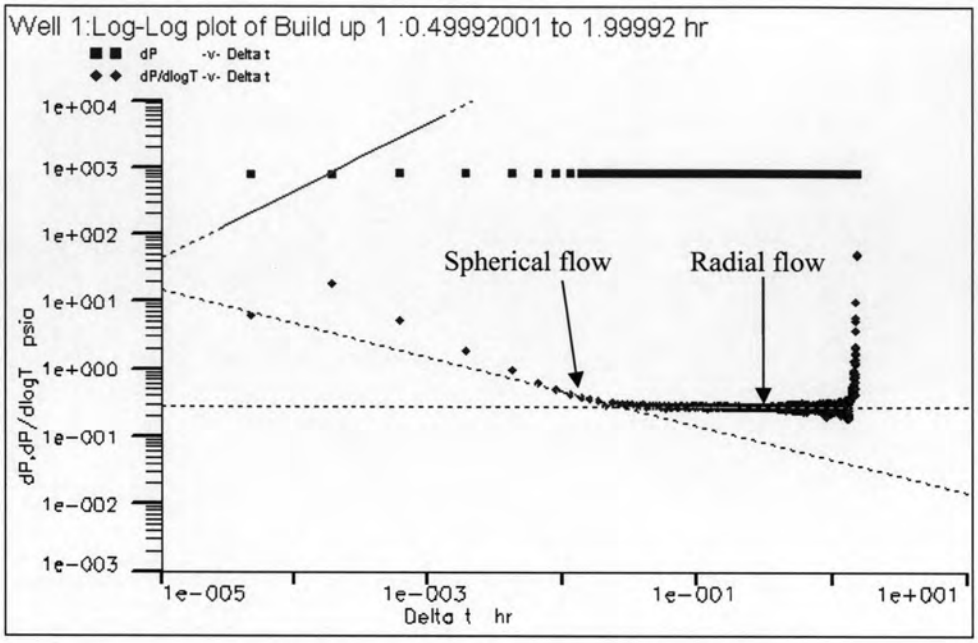

(c) Radius of stimulated zone = 1.28 ft.

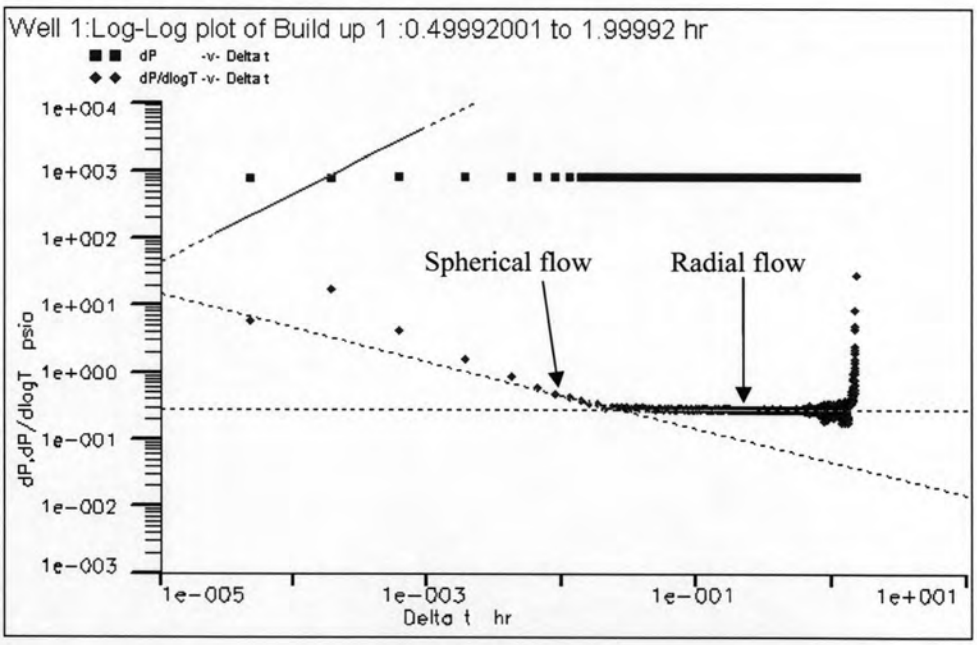

(d) Radius of stimulated zone = 3.35 ft.

Figure 7.7 : Diagnostic plots for different radii of stimulated zone for case I (continued).

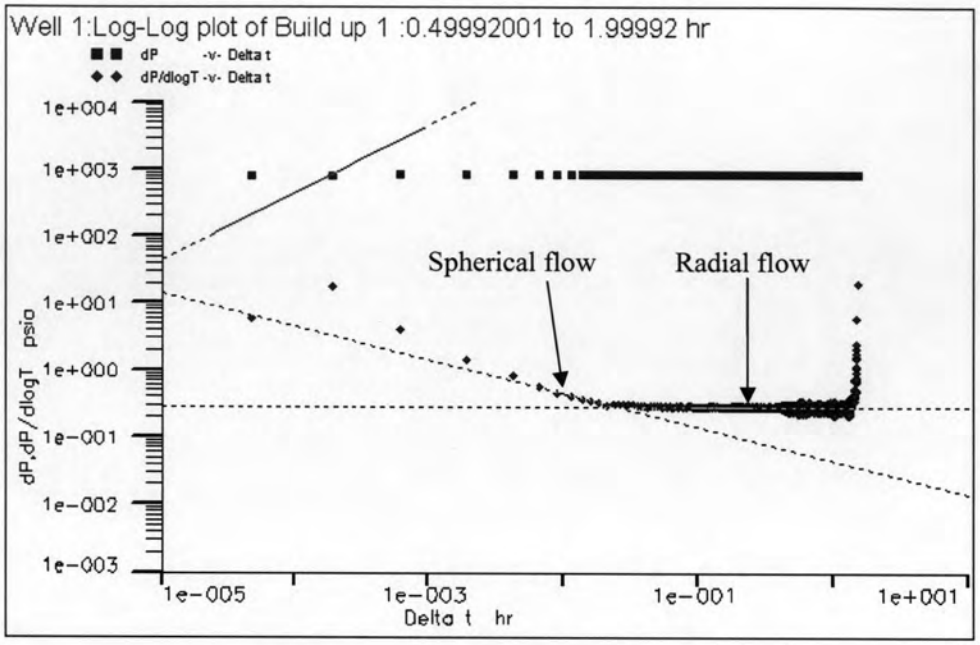

(e) Radius of stimulated zone = 4.56 ft.

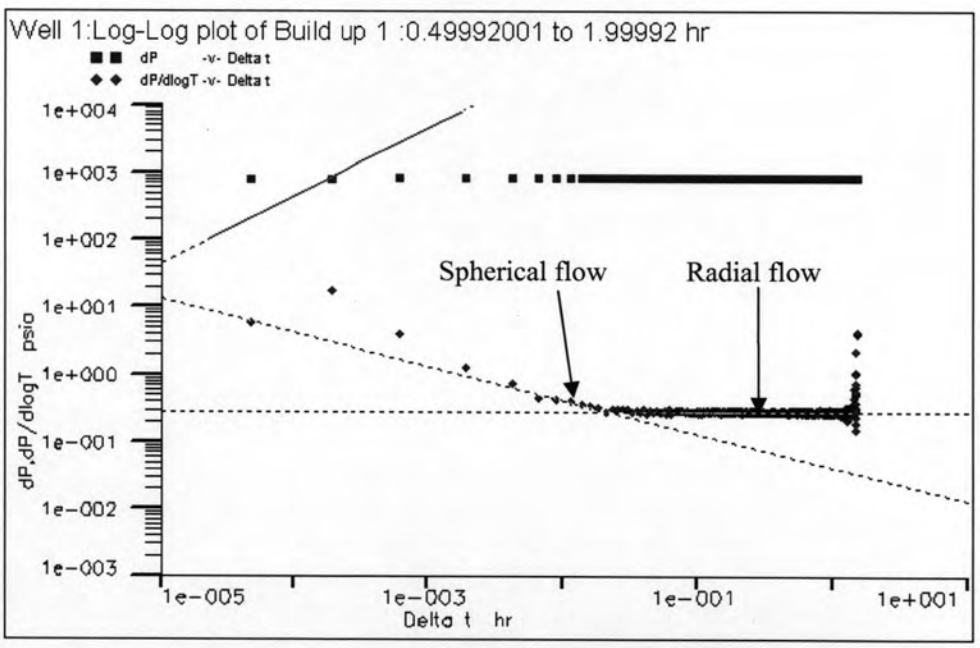

(f) Radius of stimulated zone = 6.19 ft.

Figure 7.7 : Diagnostic plots for different radii of stimulated zone for case I (continued).

Table 7.2 : Interpreted results for different radii of stimulated zone for case I.

Case	r_s	K_{hi}	K_{hu}	S_p	S_M	S_t	Interpreted results		Error %		
	(ft)	(mD)	(mD)				K_h (mD)	Skin	K_h (mD)	S_M	S_t
K75-50-1	0.44	75	50	0.299	-0.188	0.111	49.7	0.029	-0.6	115.42	-73.87
K75-50-2	0.64	75	50	0.299	-0.313	-0.014	48.3	-0.0086	-3.4	97.25	38.57
K75-50-3	1.28	75	50	0.299	-0.544	-0.245	47.9	-0.135	-4.2	75.18	44.89
K75-50-4	3.35	75	50	0.299	-0.865	-0.566	50.3	-0.062	0.6	92.83	89.04
K75-50-5	4.56	75	50	0.299	-0.967	-0.668	50.3	0.091	0.6	109.41	113.62
K75-50-6	6.19	75	50	0.299	-1.069	-0.77	48.4	0.297	-3.2	127.78	138.57

As can be seen in Figure 7.7 (a)-(f), the spherical flow model and the radial flow model can be matched with the pressure derivative plot. In Appendix B, in Figure B6 (a)-(f), the regressions show good consistency on the log-log diagnostic plot. The regression model is vertical interference test.

In this case study, we fixed the permeability of the stimulated zone and the native reservoir but varied the radius of stimulated zone. The extra pressure change or ΔP_s in the stimulated zone can be used to quantify the skin effect. The interpreted results obtained from the regression for different radii of stimulated zone are summarized in Table 7.2. It can be seen that the interpreted skin factors are overestimated compared with the mechanical skin factor, S_M. This is due to the fact that the interpreted skin factor is affected by the spherical skin or the skin due to probe, S_P as can be seen that the errors between the interpreted results and the total skin factor, S_t are reduced. For cases K75-50-5 and K75-50-6 which have large radius of invasion, the interpreted skin factors are positive, indicating damage in the reservoir. This is because when the radius of the stimulated zone goes further into the reservoir, the reservoir acts like a composite model. This means that the positive skin comes from the skin factor of the inner zone itself. Therefore, this interpreted skin factor cannot be used to define the effect from the stimulated zone. For horizontal permeability, as shown in Table 7.2 there is fluctuation of interpreted permeability between case to case due to the human error from the interpretation. However, the interpreted permeabilities are quite similar to the native reservoir permeability used in the simulation indicating that the interpreted horizontal permeability is not affected by the stimulated zone.

7.2 Case II : Undisturbed Permeability of 1 mD, Stimulated Zone Permeability of 10 mD

7.2.1 Effects of Mobility Ratio

In this case study, the objective is to investigate the effects of mobility ratio between the stimulated zone and the native reservoir on pressure transients by fixing the permeability of the native reservoir while varying the permeability of the stimulated zone. Three different mobility ratios, K_{hi}/K_{hu} of 5, 10, and 50 are considered. The native reservoir permeability is fixed at 1 mD while the stimulated zone permeability varies with the mobility ratio. The radius of stimulated zone is fixed at 11.35 ft. away from the borehole wall as shown in Figure 7.8. The flow period consists of a 100-minute drawdown and a 300-minute buildup. After running reservoir simulation for pressure response, the data were then interpreted by pressure transient analysis technique. The pressure history and the diagnostic plots of the tests are shown in Figures 7.9 and 7.10, respectively, and the interpreted results are tabultated in Table 7.3. The regression fits to the tests are shown in Appendix B.

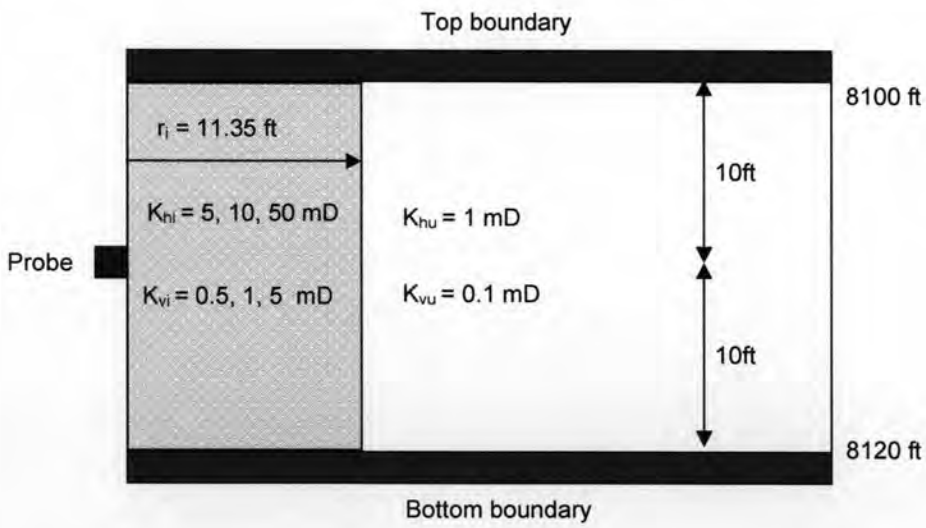

Figure 7.8 : Schematic reservoir description for different mobility ratios between stimulated zone and native reservoir for case II.

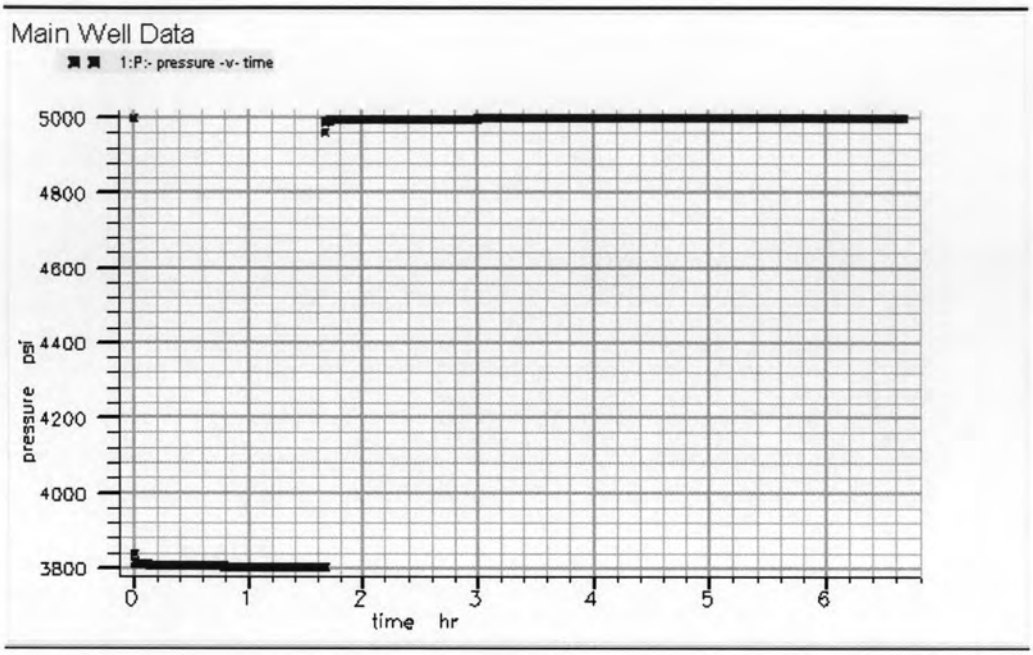

Figure 7.9 : Pressure history of case K10-1 (mobility ratio = 10)

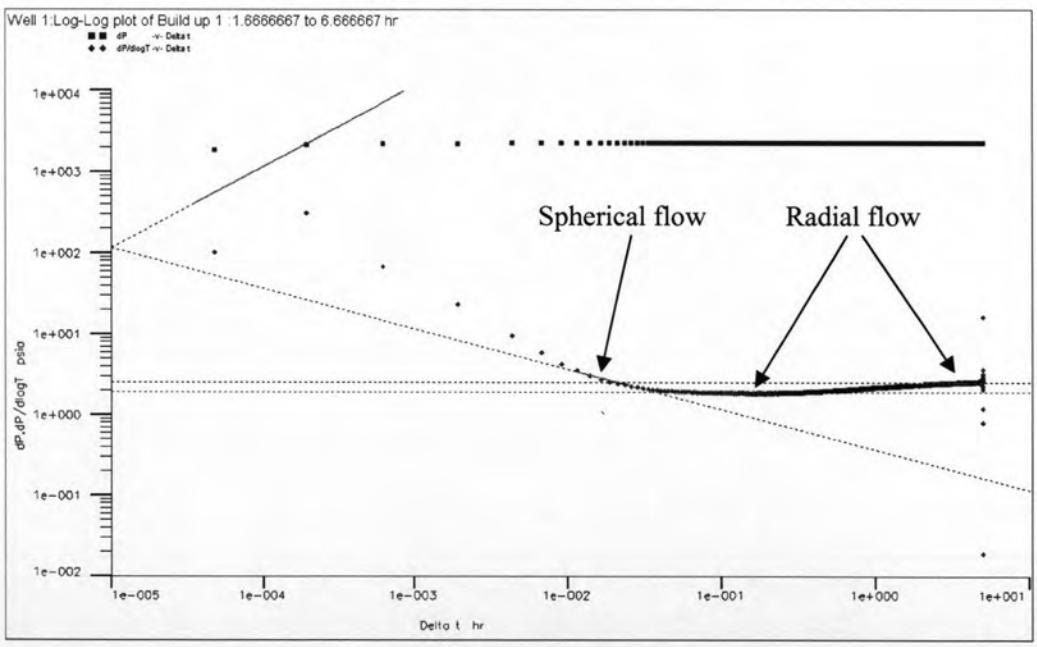

(a) Mobility ratio = 5

Figure 7.10 : Diagnostic plots for different mobility ratios between stimulated zone and native reservoir for case II.

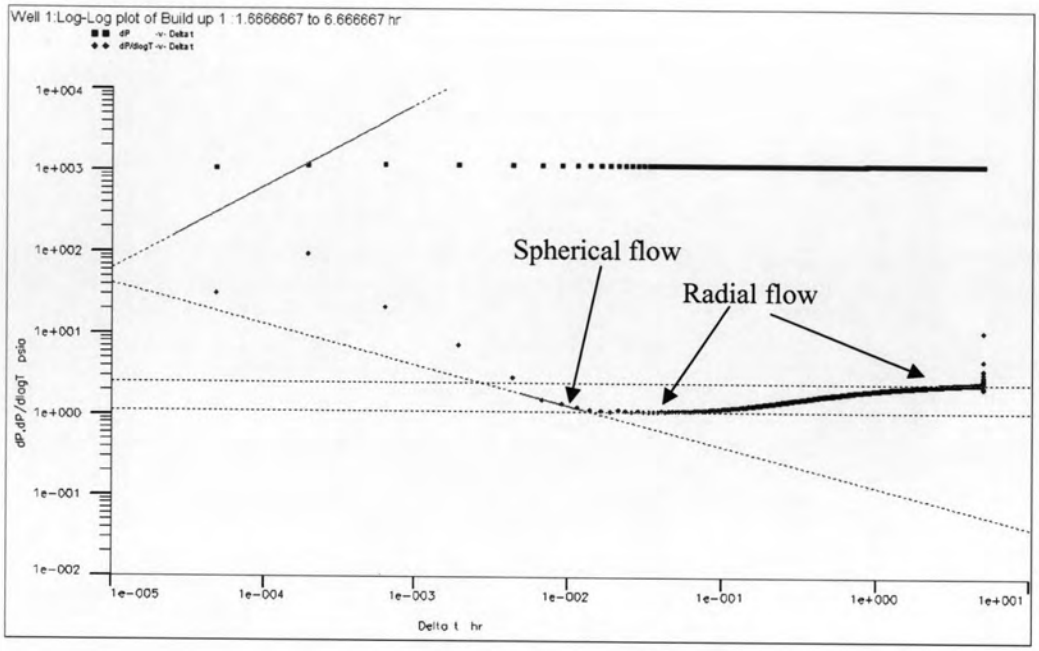

(b) Mobility ratio = 10

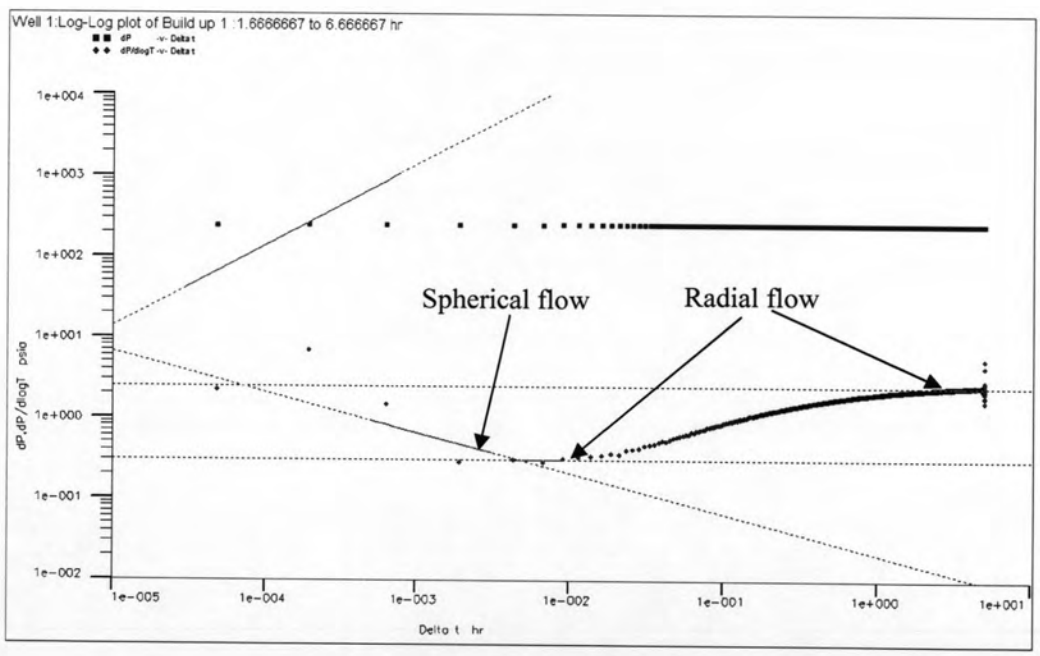

(c) Mobility ratio = 50

Figure 7.10 : Diagnostic plots for different mobility ratios between stimulated zone and native reservoir for case II (continued).

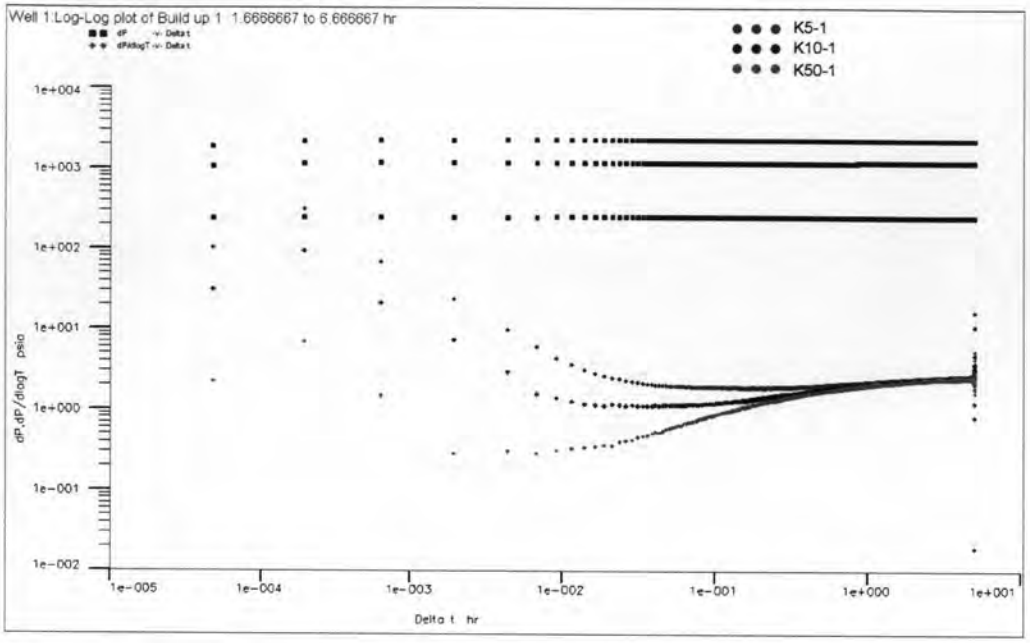

Figure 7.11 : Combination of diagnostic plots for different mobility ratios between stimulated zone and native reservoir for case II.

Table 7.3 : Interpreted results for different mobility ratios between stimulated zone and native reservoir for case II.

Case	K_{hi} (mD)	K_{xyzi} (mD)	K_{hu} (mD)	K_{xyzu} (mD)	Interpreted results				Error %			
					K_{hi} (mD)	K_{xyzi} (mD)	K_h (mD)	K_{xyzu} (mD)	K_{hi} (mD)	K_{xyzi} (mD)	K_h (mD)	K_{xyzu} (mD)
K5-1	5	2.321	1	0.464	1.496	2.657	1.112	-	-70.08	14.47	11.2	-
K10-1	10	4.640	1	0.464	2.499	3.981	1.122	-	-75.01	-14.20	12.2	-
K50-1	50	23.21	1	0.464	9.366	13.38	1.146	-	-81.26	-42.35	14.6	-

From the pressure history plot shown in Figure 7.9, the pressure drop is high enough to reduce the noise. So, in this case study, the effect from noise due to too small pressure drop goes away.

As can be seen in the diagnostic plots in Figure 7.10 (a), (b), and (c), the spherical flow model can be matched with the data during the period before the flow regime change to radial flow corresponding to the inner or stimulated zone. After that, the flow regime changes to radial flow again corresponding to the outer or native reservoir.

In this case study, the regression fits on the data are quite poor as can be seen in Appendix B, Figure B7 (a), (b), and (c). Since cases K5-1, K10-1, and K50-1 have the radius of stimulated zone of 11.35 ft. which is too large to act like a stimulated zone. So, the reservoir behaves like a composite model. But our regression model is simple vertical interference test. Therefore, to make the regression better match with the data, we need the correct regression model which is a single probe with composite reservoir model. However, the required model is not available at this time.

In this case study, we fixed the radius of stimulated zone but varied the permeability in the stimulated zone. As expressed earlier that the regression model is not correct model, the skin factor cannot be correctly estimated. The radius of the stimulated zone is large enough to see the change in mobility and the horizontal permeability of both the inner or stimulated zone and the outer or native reservoir can be estimated. The interpreted horizontal permeabilities of the inner zone are much less than the input value but interpreted horizontal permeabilities of the outer zone are quite similar to the input value. Thus, for stimulated reservoir, the horizontal permeability of the native reservoir can be interpreted with an accurate result. In Table 7.3, for cases K5-1 and K10-1, spherical permeability of the inner zone, the interpreted results are quite similar to the input value but for case K50-1, the error is large because the period of the spherical flow regime is too short.

As can be seen in the combination of diagnostic plots in Figure 7.11, at time between 0.01 hr and 0.1 hr, the pressure derivative plot represents the flow regime in the inner or stimulated zone. And at late time, after 0.1 hr, the pressure derivative plot represents the flow regime in the outer or native reservoir. At the middle time, the pressure derivative plot of case K10-1 (blue line) is under the pressure derivative plot of case K5-1 (red line) and the pressure derivative plot of case K50-1 (green line) is lower than those of cases K5-1 and K10-1. This behavior is practical because the lower line stand for higher mobility.

7.2.2 Effects of Radius of Stimulated Zone

In this case study, the objective is to investigate the effects of radius of the stimulated zone on pressure transients by fixing the permeability of the stimulated zone and the native reservoir while varying the stimulated zone radius as depicted in Figure 7.12. Eight different radii of stimulated zones, r_s of 0.44, 0.64, 1.28, 3.35, 4.56, 6.19, 11.35, and 20.71 ft. are considered. The native reservoir permeability is fixed at 1 mD, and the stimulated zone permeability is fixed at 10 mD. The flow period consists of a 100-minute drawdown and a 300-minute buildup. After running reservoir simulation for pressure response, the data were then interpreted by pressure transient analysis technique. The pressure history and the diagnostic plots of the tests are shown in Figures 7.13 and 7.14, respectively, and the interpreted results are tabulated in Table 7.4. The regression fits to the tests are shown in Appendix B.

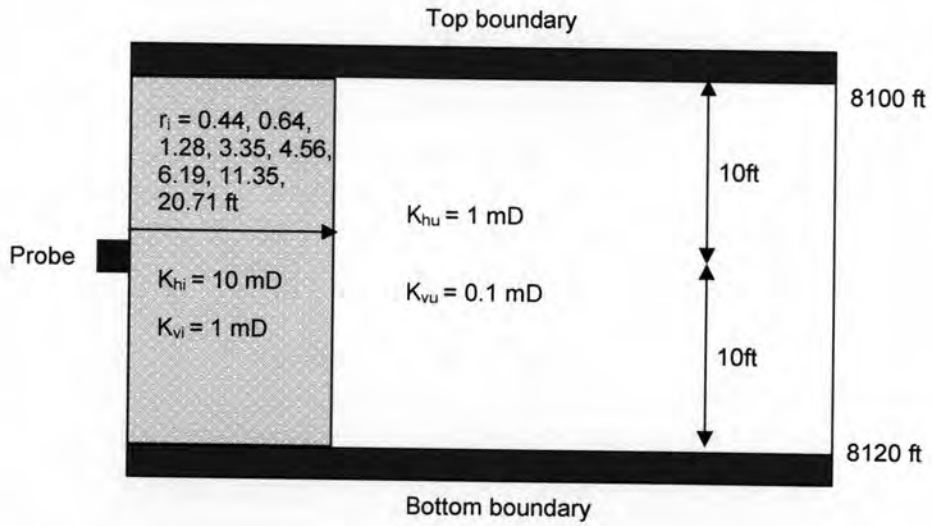

Figure 7.12 : Schematic reservoir description for different radii of stimulated zone for case II.

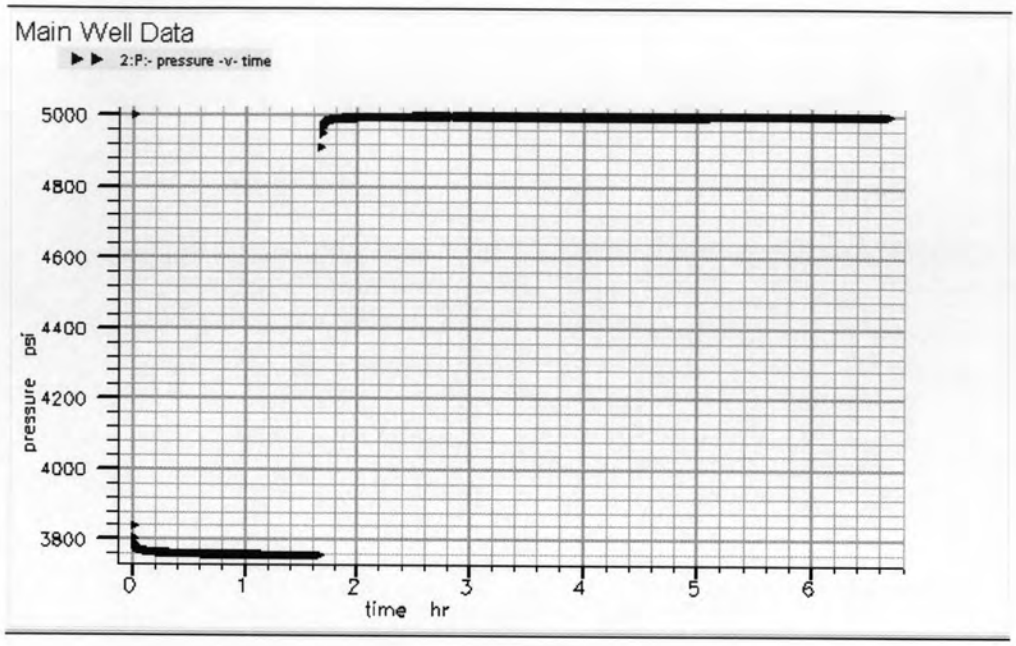

Figure 7.13 : Pressure history for case K10-1-3 (radius of stimulated zone = 1.28 ft.)

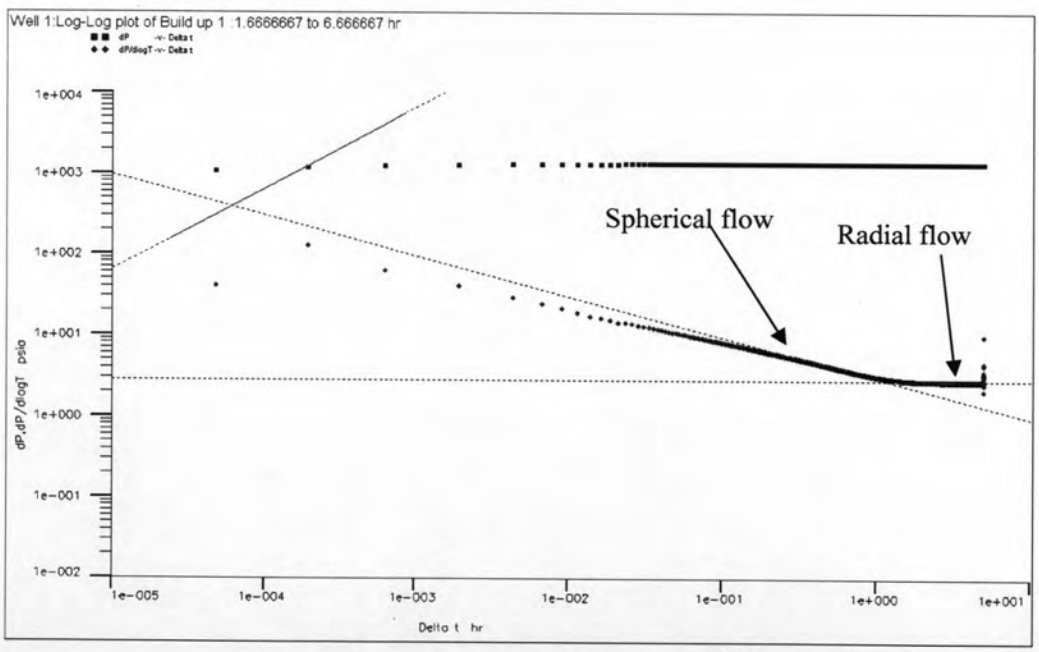

(a) Radius of stimulated zone = 0.44 ft.

Figure 7.14 : Diagnostic plots for different radii of stimulated zone for case II.

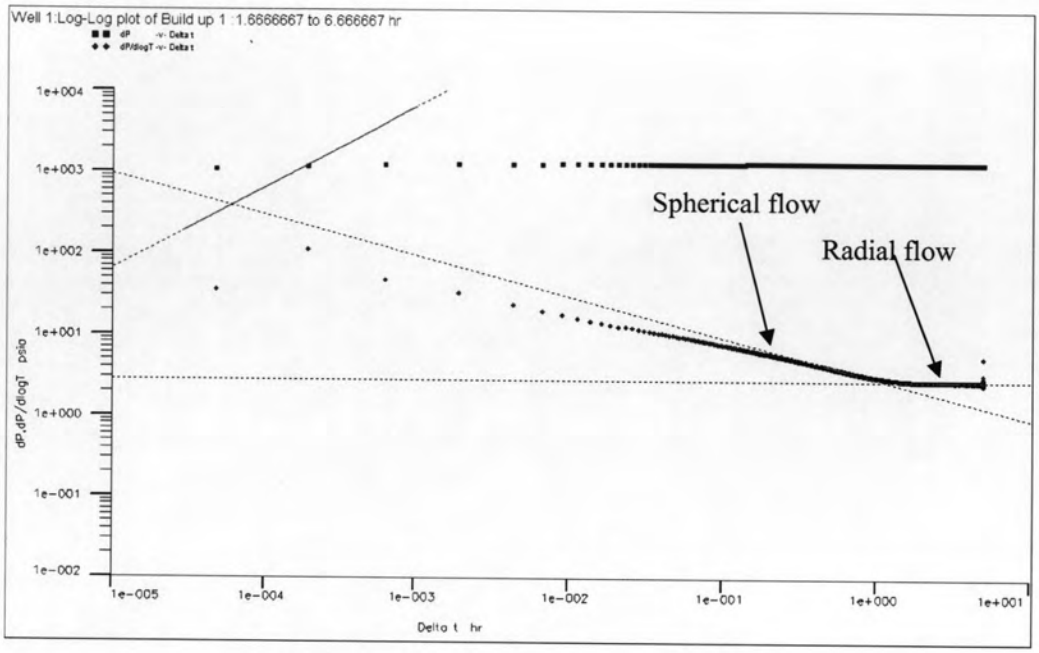

(b) Radius of stimulated zone = 0.64 ft.

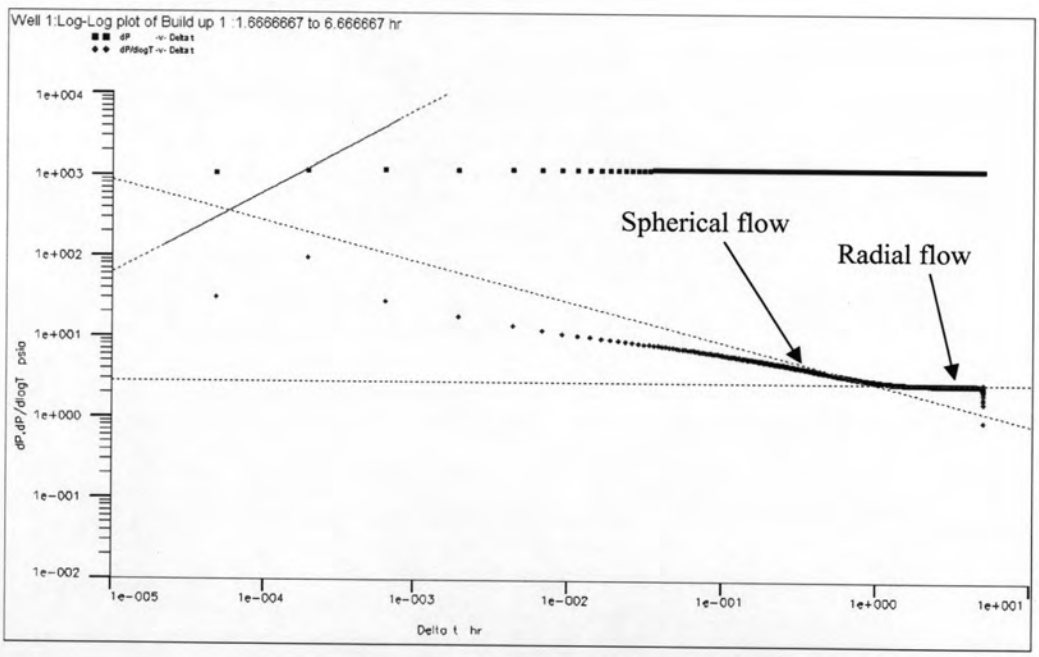

(c) Radius of stimulated zone = 1.28 ft.

Figure 7.14 : Diagnostic plots for different radii of stimulated zone for case II (continued).

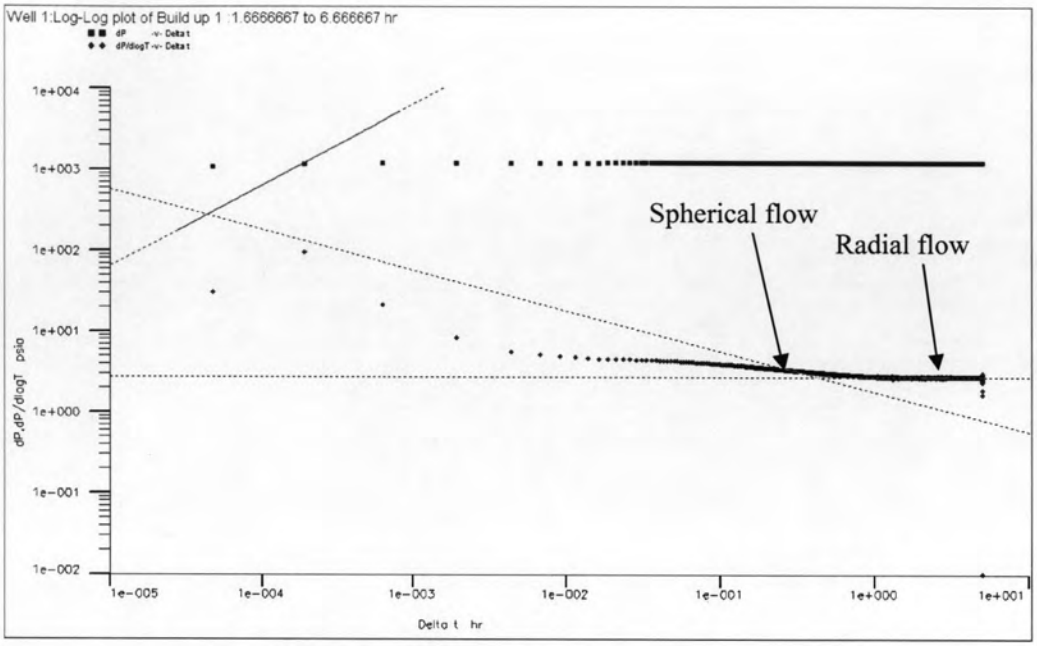

(d) Radius of stimulated zone = 3.35 ft.

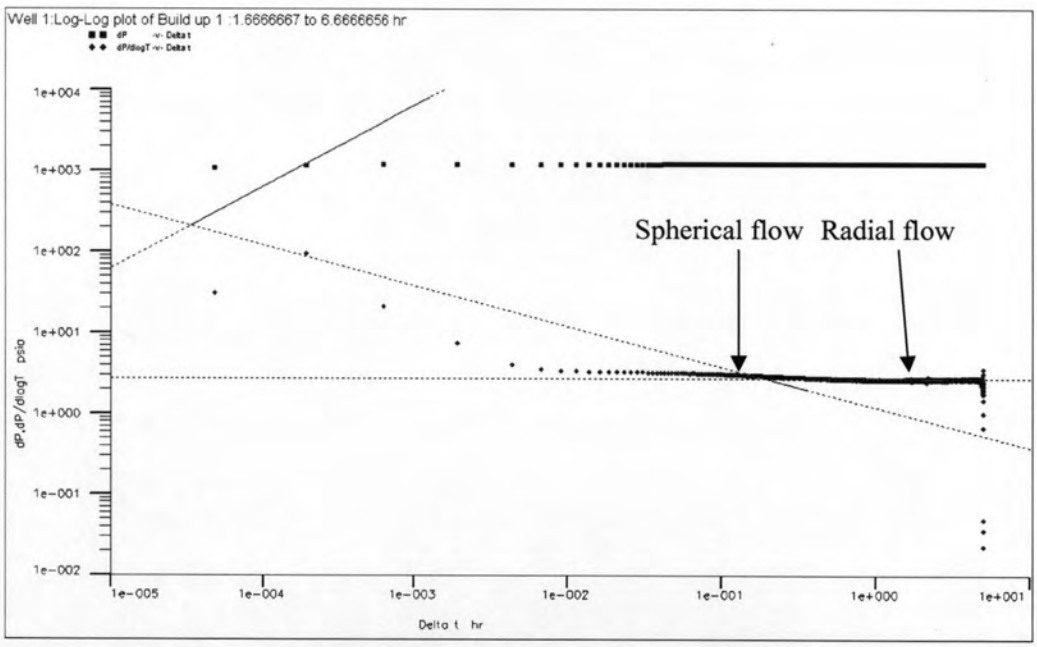

(e) Radius of stimulated zone = 4.56 ft.

Figure 7.14 : Diagnostic plots for different radii of stimulated zone for case II (continued).

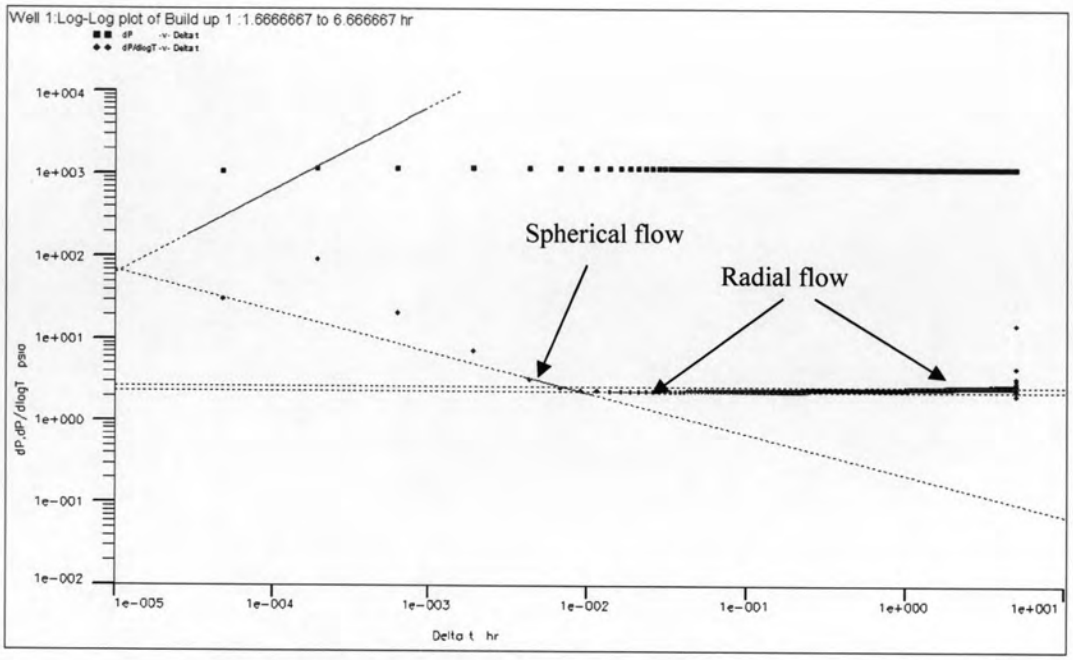

(f) Radius of stimulated zone = 6.19 ft.

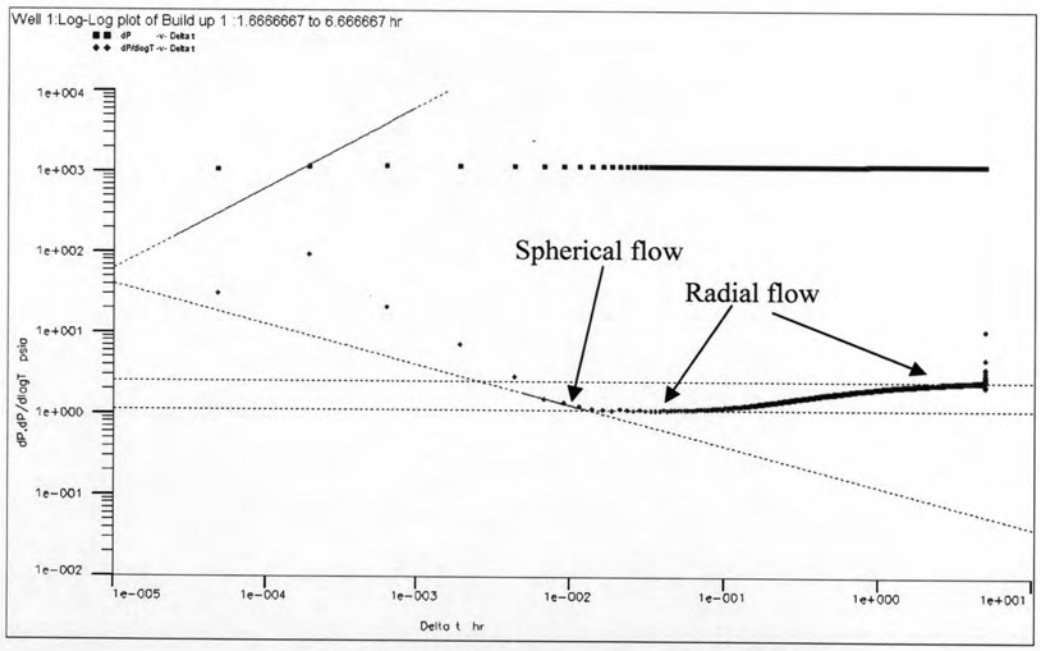

(g) Radius of stimulated zone = 11.35 ft.

Figure 7.14 : Diagnostic plots for different radii of stimulated zone for case II (continued).

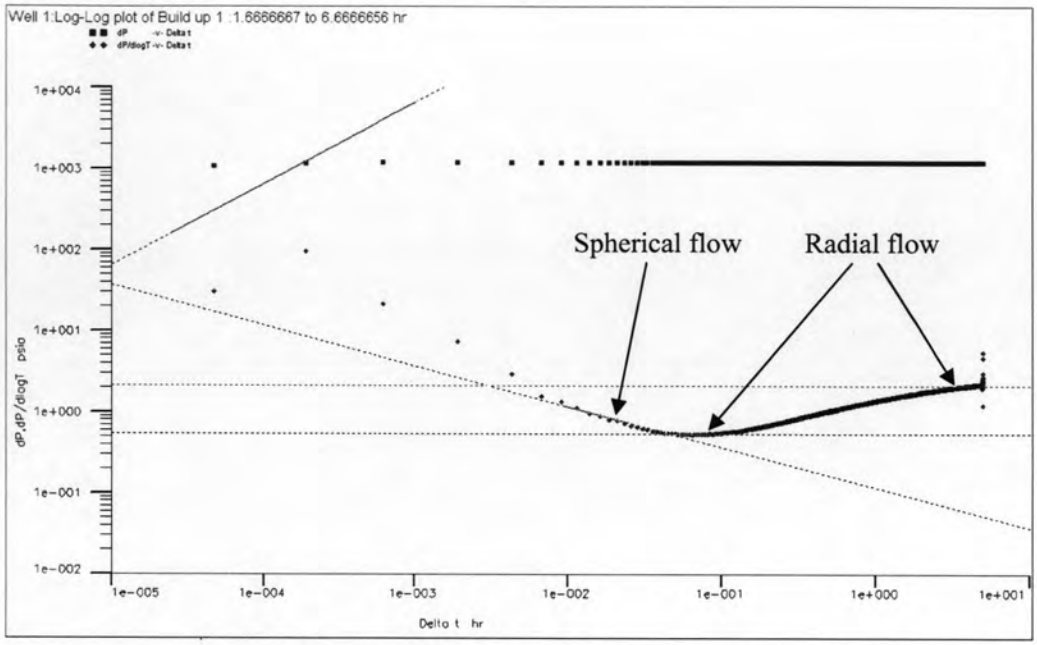

(h) Radius of stimulated zone = 20.71 ft.

Figure 7.14 : Diagnostic plots for different radii of stimulated zone for case II (continued).

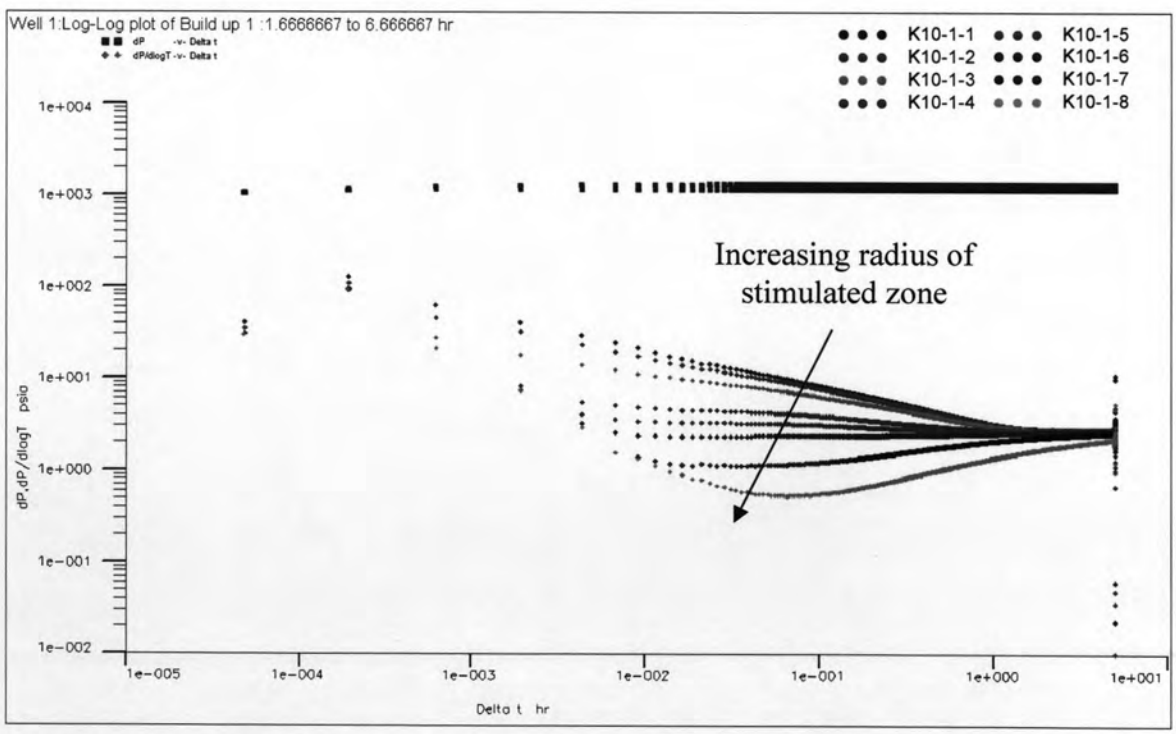

Figure 7.15 : Combination of diagnostic plots for different radii of stimulated zone for case II.

Table 7.4 : Interpreted results for different radii of stimulated zone for case II.

Case	r_i (ft)	K_{hi} (mD)	K_{xyzi} (mD)	K_{hu} (mD)	K_{xyzu} (mD)	Interpreted results				Error %			
						K_{hi} (mD)	K_{xyzi} (mD)	K_h (mD)	K_{xyzu} (mD)	K_{hi} (mD)	K_{xyzi} (mD)	K_h (mD)	K_{xyzu} (mD)
K10-1-1	0.44	5	2.924	1	0.464	-	-	1.023	0.483	-	-	2.3	4.09
K10-1-2	0.64	5	2.924	1	0.464	-	-	1.024	0.494	-	-	2.4	6.47
K10-1-3	1.28	5	2.924	1	0.464	-	-	1.026	0.545	-	-	2.6	14.75
K10-1-4	3.35	5	2.924	1	0.464	-	-	1.037	0.693	-	-	3.7	49.35
K10-1-5	4.56	5	2.924	1	0.464	-	-	1.05	0.908	-	-	5.0	95.69
K10-1-6	6.19	5	2.924	1	0.464	1.203	2.787	1.064	-	-75.94	-4.68	6.3	-
K10-1-7	11.35	5	2.924	1	0.464	2.499	3.981	1.122	-	-50.02	36.15	12.2	-
K10-1-8	20.71	5	2.924	1	0.464	4.256	5.243	1.351	-	-14.88	79.31	35.1	-

From the pressure history plot shown in Figure 7.13, the pressure drop is high enough to reduce the noise. So, in this case study, the effect from noise due to too small pressure drop goes away.

For small radius of stimulated zone, cases K10-1-1, K10-1-2, K10-1-3, K10-1-4, and K10-1-5 as shown in Figure 7.14 (a), (b), (c), (d), and (e), the pressure derivative plots show homogeneous reservoir but when increasing the radius of the stimulated zone, the pressure derivative tends to move downward as can be seen more obviously in Figure 7.15.

For large radius of stimulated zone, cases K10-1-6, K10-1-7, and K10-1-8 as shown in Figure 7.14 (f), (g), and (h), the pressure derivative plots indicate composite reservoir model. The single probe tool encountered a high mobility zone before changing the mobility to low mobility zone.

In Figure 7.14 (a), (b), and (c), the spherical flow model can be matched with the data corresponding to the outer or native reservoir before the flow regime change to radial flow also corresponding to the outer zone. For the inner zone, the flow regime cannot be detected. For cases K10-1-4 and K10-1-5 in Figure 7.14 (d) and (e), the spherical flow model of the outer zone is hard to match with the data but the radial flow model of the outer zone can match with data. For cases K10-1-6, K10-1-7, and K10-1-8 in Figure 7.14 (f), (g), and (h), the detected spherical flow regime comes from the inner zone and the radial flow can be detected from both the inner and outer zones.

In Appendix B, Figure B8 (a), and (b), the regression plot of small radius of stimulated zone (cases K10-1-1 and K10-1-2) shows reasonable match with the data

particularly in the middle to late time. For large radius of stimulated zone cases (K10-1-3, K10-1-4, K10-1-5, K10-1-6, K10-1-7, and K10-1-8) shown in Figure B10 (c), (d), (e), (f), (g), and (h), the regression plots show poor match with the data. This is due to the fact that when the permeability contrast between the inner zone and the outer zone is high and the radius of stimulated zone is large, the reservoir behaves like a composite model. But our regression model is simple vertical interference test. Therefore, to make the regression better match with the data, we need the correct regression model which is the single probe with composite reservoir model. However, the required model is not available at this time.

In this case study, we fixed the permeability of the stimulated zone and permeability of the native reservoir but varied the radius of stimulated zone. As expressed earlier, the regression model is not the correct model, so the skin factor cannot be estimated. The interpreted results obtained from the graphical analysis for different radii of stimulated zone are summarized in Table 7.4. For cases K10-1-1, K10-1-2, K10-1-3, K10-1-4, and K10-1-5, the interpreted horizontal permeability is quite similar to the input value of native reservoir horizontal permeability. For interpreted spherical permeability, the error increases when the radius of stimulated zone increases because the spherical flow model does not match well with the data on the derivative plot as can be seen in Figure 7.14 (d) and (e). For cases K10-1-6, K10-1-7, and K10-1-8, the spherical and horizontal permeability of the inner zone can be interpreted. The error from interpreted spherical and horizontal permeability is high because the radial flow regime of the inner zone is still not fully developed. Thus, if the radius of stimulated zone is not high, the spherical and horizontal permeability of the inner zone can not be interpreted accurately.